

Synthesis and characterization of a slow-release fertilizer produced from coconut husk biochar

A. T. Sojan¹, J. K. Smitha^{1*}, T. Geetha²

¹Department of Soil Science and Agricultural Chemistry, College of Agriculture, Kerala Agricultural University, Thrissur – 680656, Kerala, India

²Department of Chemistry, Vimala College (Autonomous), Thrissur – 680009, Kerala, India

Revised: February 23, 2025

Coconut biochar-based multi-nutrient fertilizer (CBMNF) was synthesized by first converting coconut husk to coconut biochar (CB) through pyrolysis. The essential nutrients like nitrogen, zinc, iron, manganese, copper, boron and molybdenum were impregnated onto the biochar matrix through adsorption to synthesize CBMNF. Nutrient levels increased significantly after adsorption, with carbon and nitrogen percentages rising from 56.86 and 0.147 % to 71.57 and 0.27 %, respectively. Additionally, micro-nutrients zinc, iron, manganese, copper, and boron in CB increased from 76, 343.21, 106, 30, and 52.29 mg kg⁻¹ to 885, 1575, 328, 66, and 191.42 mg kg⁻¹, respectively, confirming successful nutrient impregnation into the biochar. This was further confirmed by shift in peak position observed in FTIR spectra and the reduction in pore size due to surface deposition of nutrients observed in SEM. TGA showed improved thermal stability of CBMNF in comparison to CB. Dissolution study in the soil further revealed its ability to gradually release essential macro and micronutrients, underscoring its slow-release capability. Hence, CBMNF may effectively replace or supplement traditional chemical fertilizers in agriculture.

Keywords: coconut husk, biochar, multi-nutrient-fertilizer, slow-release fertilizer, thermal stability, dissolution study

INTRODUCTION

Coconut is an essential perennial crop with multiple uses that supports life in vulnerable coastal and island habitats [1]. It is cultivated in around 80 countries, yielding a total global production of 69.8 billion nuts with Sri Lanka, Indonesia, Philippines, and India being the major producers [2].

Coconut husk contains 70 g of pith and 30 g of fiber [3]. Although coconuts are produced in vast quantities in different parts of the world and coconut husks is abundantly available, only about 28% of the coconut husks produced is used in coir industry. The rest is often discarded as a waste due to its lack of economic value. A sizable portion is found submerged in the fields as a cultural tradition, and the rest often burnt [4]. A better alternative is the conversion of agricultural wastes like coconut husks into valuable products by adopting modern technologies. Therefore, organic waste conversion via decomposition is crucial for Resource management and sustainable agriculture [5].

Biochar produced from waste materials like coconut husk by pyrolysis is a beneficial product with many useful characteristics [6]. Biochar application in soil has gained momentum because of economic and ecological benefits like improving soil remediation and increased carbon sequestration [7].

It also improves soil fertility and soil health [8].

In contrast, the conventional chemical fertilizers, being soluble in water, are readily washed off and leached from soil. Approximately 40-70% of N, 80-90% of P, and 50-70% of K fertilizers are estimated to have been lost to the environment. The phenomenon not only seriously pollutes environment and threatens sustainable agriculture, it also results in significant economic loss to farmers. Furthermore, overuse of chemical fertilizers seriously deteriorates farming lands by reducing organic matter and salinizing the soil [9]. The awareness about slow-release fertilizers (SRFs), which are intentionally designed to address the shortcomings of conventional fertilizers, is now widespread. SRFs release nutrients more slowly than conventional fertilizers, extending their supply of nutrients without environmental problems.

Biochar with its unique characteristics, may be used as such or modified to develop slow-release-fertilizer. Techniques like impregnation, pelletization, and encapsulation were developed in the last decade to fabricate nutrient-loaded biochar [10-12]. In addition to reducing greenhouse gas emissions, they may modify pH of soil, increase soil permeability, decrease bulk density, sequester soil carbon and increase crop yields [13-15].

* To whom all correspondence should be sent:
E-mail: smithajohn.k@kau.in

Though studies on biochar derived from coconut husks exist in literature, the novelty of the present study is the enrichment of the prepared biochar with multi-nutrients, viz. nitrogen, zinc, copper, boron, iron, manganese & molybdenum, to synthesise a slow-release fertilizer. Since nutrient-enriched coconut husk biochar is derived from a widely available and inexpensive agro-waste, it effectively addresses the problem of waste management in agricultural land. Further, as the nutrients embedded in biochar are slowly released, it also addresses the problem of rapid release of nutrients and its consequent loss associated with conventional fertilizers.

MATERIALS AND METHODS

Preparation of coconut biochar

Coconut husk, the raw material used to synthesize coconut biochar (CB), was collected locally from Thrissur district, Kerala and subjected to pyrolysis at 330°C over a 24 h duration. The biochar produced was crushed into extremely fine particles and then passed through a 2mm sieve to obtain uniform particle size. The final product was sealed in airtight plastic bags for future use.

Preparation and stability analysis of multi-nutrient mixture

Different analytical reagent (AR)-grade chemicals, including urea ($\text{CO}(\text{NH}_2)_2$), zinc sulfate ($\text{ZnSO}_4 \cdot \text{H}_2\text{O}$), boric acid (H_3BO_3), copper sulfate ($\text{CuSO}_4 \cdot 5\text{H}_2\text{O}$), ferrous sulfate ($\text{FeSO}_4 \cdot 7\text{H}_2\text{O}$), manganese sulfate ($\text{MnSO}_4 \cdot 7\text{H}_2\text{O}$), and molybdenum trioxide (MoO_3), were purchased from Merck India Private Limited. These chemicals were blended to achieve the desired nutrient composition, that is, N (7.5%), Zn (6%), B (4%), Cu (0.02%), Fe (0.02%), Mn (0.25%) and Mo (0.01%) in the multi-nutrient mixture. The stability and quality of the prepared MNM were checked by regularly monitoring color, clumping tendency, solubility, pH and EC over a six-month period.

Synthesis of coconut biochar-based multi-nutrient fertilizer

The coconut biochar-based multi-nutrient fertilizer (CBMNF) was prepared by impregnating nutrients into the biochar. Ten g of biochar and 0.5 g of nutrient mix were added to 100 ml of water in a conical flask. This mixture was shaken on a rotary shaker for three h at room temperature. The substrate (CBMNF) was then filtered, oven-dried for 24 h at 105°C and later sealed in air tight plastic containers for further use.

Characterization of CB and CBMNF

- Physicochemical and electrical properties of CB. The pH, electrical conductivity (EC), moisture content, and ash percentage of the biochar were estimated using standard procedures [16, 17].
- Elemental composition & nutrient content. Analysis of carbon (C), hydrogen (H), nitrogen (N), and sulfur (S) was conducted utilizing a CHNS analyzer, specifically the Elementary Vario EL cube model. Additionally, the total nutrient content of zinc (Zn), iron (Fe), manganese (Mn), copper (Cu), and boron (B) was determined by first digesting the sample using a nitric-perchloric acid (9:4) digestion method [18] and then analyzing it using inductively coupled plasma–optical emission spectrometer (ICP-OES; Model: Optima® 8×00 series).
- Microstructural and chemical analyses. The biochar's surface morphology was examined utilizing a field emission scanning electron microscopy (SEM) tool, namely the Joel 6390LA/OXFORD XMX N SEM-EDAX system. Functional group analysis of the biochar was performed using Fourier transform infrared (FT-IR) spectroscopy, employing Perkin Elmer Spectrum IR instrument. For the identification of phases and determination of crystallinity, X-ray diffraction (XRD) was performed using the Aeris XRD diffractometer from Malvern Panalytical. To assess the thermal stability of the biochar, thermogravimetric analysis (TGA) was carried out utilizing the TGA-DTA Perkin Elmer STA6000 instrument.

Water retention (WR) of CBMNF

For the water retention (WR) study, pre-weighed cups were utilized. Cup A served as the control or blank and was filled with 50 g of sieved soil. Cup B contained 2 g of nanocomposite and 50 g of soil. Then, distilled water (30 mL) was added to both cups. After 24 h, the cups were reweighed (as W_{A1} and W_{B1}). Subsequently, the cups were placed in a glass box, and their weights were measured daily for 30 days (referred to as W_{A2} and W_{B2}) [19]. The water retention was determined using the following equation:

$$WR (\%) = \frac{W_A}{W_B} \times 100 \text{-----(1)}$$

Nutrient release study in soil

The experiment followed a completely randomized design (CRD). To evaluate the nutrient release from the substrate in soil, a PVC column measuring 30 cm in length and 10 cm in diameter was employed. The columns were filled with soil

(2.5 kg), soil + CBMNF (2.5 kg of soil and 62.5 g of CBMNF) and soil + nutrient mix (2.5 kg of soil and 6.25 g of nutrients), respectively. The soil was first saturated to attain field capacity and then left to stabilize for 3 days. Hundred mL of de-ionized water was added to the column every 24 h for 60 days. Leachate was collected at specific intervals of 1, 2, 3, 5, 10, 15, 30, 45, and 60 days and analyzed to determine the concentrations of N, Zn, Fe, Mn, Cu, B and Mo.

RESULTS AND DISCUSSION

Stability analysis of multi-nutrient mixture

No color change and caking of the mixture was observed on storage. It is readily soluble in de-ionized water and neither pH nor EC varied over time. Thus, the mixture has excellent stability and keeping quality and can be safely stored for at least six months.

Characterization of CB and CBMNF

The coconut biochar-based multi-nutrient fertilizer was synthesized by impregnating the nutrients onto the biochar. During this impregnation, all the nutrients, viz., N, Zn, Fe, Mn, Cu, B, and Mo, were adsorbed onto the biochar. The adsorption of nutrients onto biochar may be either physical or chemical or both. The extent to which nutrients are adsorbed on the biochar is influenced by various factors like covalent forces between the adsorptive biochar and nutrient, chelating reaction between adsorbent & adsorbate, controlled ion exchange, etc. [20, 21].

- Physicochemical and electrical properties. The moisture content, ash content, pH and EC of CB and CBMNF are given in Table 1. The ash content, pH and EC of CBMNF were lower than those of BC while the moisture content was higher. CB & CBMNF are alkaline in aqueous solution, probably due to the presence of basic cations (Na, K, Ca & Mg) and their compounds like salts (chlorides), oxides, hydroxides, and carbonates [22-24]. During the synthesis of CBMNF, for adsorbing the multinutrients on to biochar, biochar & multinutrient mix are shaken together in an aqueous medium. This could have led to the depletion of readily soluble salts, soluble alkaline cations, and fine ash resulting in lower pH values, EC values and reduced ash content in CBMNF [25, 26]. The pH & EC of CBMNF were lower than those of BC by 0.87 & 1.73 units, respectively. The ash content was lower by 56% while the moisture content was higher by 34%.

Table 1. Electrochemical properties of CB and CBMNF

Parameters	CB	CBMNF
Moisture (%)	10.42	15.8
Ash (%)	23.97	10.64
pH	9.48	8.61
EC (dS m ⁻¹)	3.46	1.73

- Elemental composition & nutrient content. The nutrient content of CB and CBMNF is given in Table 2. The three major constituents of biochar are carbon, hydrogen and nitrogen. This is unsurprising as biochar is mostly composed of cellulose, hemicelluloses and lignin polymers. The high carbon content of BC indicates the presence of organic plant residues like cellulose and lignin in BC [27, 28]. After conversion of CB to CBMNF, the carbon content increased by 25.8 % and nitrogen content by 15.8 %. This suggest successful incorporation of urea in CBMNF. The sulfur content increased by 83.7 %, possibly due to the incorporation of sulfate on to biochar. Additionally, micro-nutrients such as zinc, iron, manganese, copper, and boron are present in CB at 76, 343.21, 106, 30 and 52.29 mg kg⁻¹ respectively. In CBMNF, these values are notably higher, with zinc at 885 mg kg⁻¹, iron at 1575 mg kg⁻¹, manganese at 328 mg kg⁻¹, copper at 66 mg kg⁻¹, and boron at 191.42 mg kg⁻¹. Comparing CBMNF to BC, an overall increase in nutrient content was observed, indicating that it has effectively adsorbed nutrients from solution.

Table 2. Elemental properties of CB and CBMNF

S. No.	Elements		CB	CBMNF
1	C	%	56.86	71.57
2	H		1.58	3.22
3	N		0.38	0.44
4	S		0.147	0.27
8	Zn	mg kg ⁻¹	76	885
9	Fe		343.21	1575
10	Mn		106	328
11	Cu		30	66
12	B		52.29	191.42

- Microstructural and chemical analyses. The biochar's morphology from SEM micrographs at 10 μm and 2 μm magnification (Fig. 1a and b) shows that CB has a honeycomb-like appearance and a well-developed porous structure.

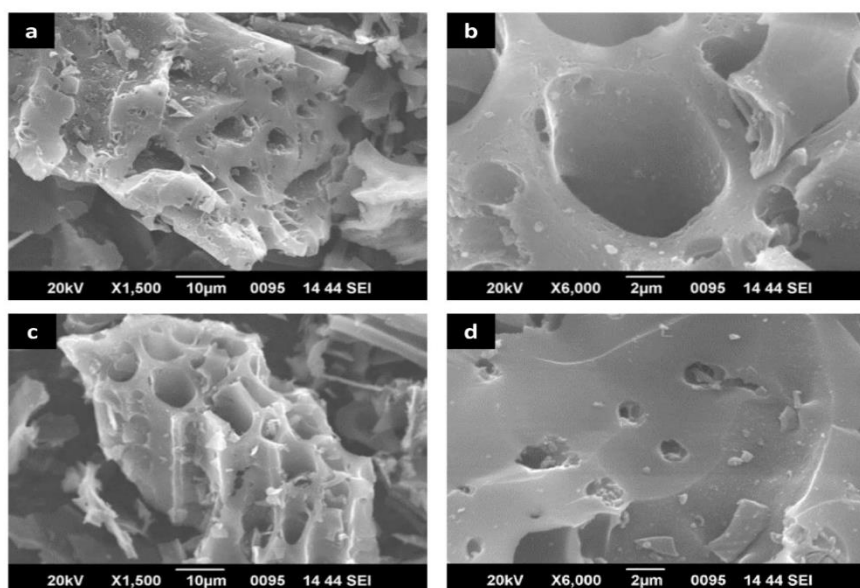


Fig. 1. SEM micrographs of coconut biochar (a) 10 μ m, (b) 2 μ m and CBMNF (c) 10 μ m, (d) 2 μ m

The porosity is due to the rapid volatilization of organic components from the plant matter during the pyrolysis phase and is beneficial for the attachment of metal ions [29]. The SEM micrographs depicting CBMNF are given in Fig. 1c and 1d. A comparison between CBNMF and CB revealed the variations in pore structures between these samples. The decrease in pore size of the CBMNF was due to the deposition of nutrients within the pores of biochar as suggested in previous studies [30]. This indicated successful deposition of nutrients onto the surface of CB thus converting it to CBMNF.

The FT-IR spectra of CB (Fig. 2a) exhibited peaks within the range of 750-1600 cm^{-1} . A weak broad low-intensity band was observed in the 3600-3400 cm^{-1} region. This might be assigned to the hydroxyl group (OH) present on the biochar's surface. Polymeric alcohol, phenol and carboxylic acid groups, possibly originating from cellulose or hemicellulose and from adsorbed water molecule, may be responsible for this peak. The band due to N-H stretching of amines also appeared in this region [31-33]. A narrow band at 1565 cm^{-1} can be attributed to the C=C-C stretching vibrations of aromatic rings probably originating from lignin [34-36]. The weak absorption band at 1359 cm^{-1} might be due to OH bending in phenols possibly formed by the transformation of lignin [37]. A broad band appearing at 1100-1000 cm^{-1} could be associated with the C-O-C stretching of the ethers in lignin or the asymmetric stretching of Si-O-Si [38]. The peak at 874 cm^{-1} might be attributed to stretching vibration of C-H [39] and the peak at 806 cm^{-1} is likely attributed to the symmetrical stretching of Si-O-Si [40]. The peak at 755 cm^{-1} might be due to out-of-

plane ring deformation or weak vibrational $-\text{CH}_2$ rocking [38].

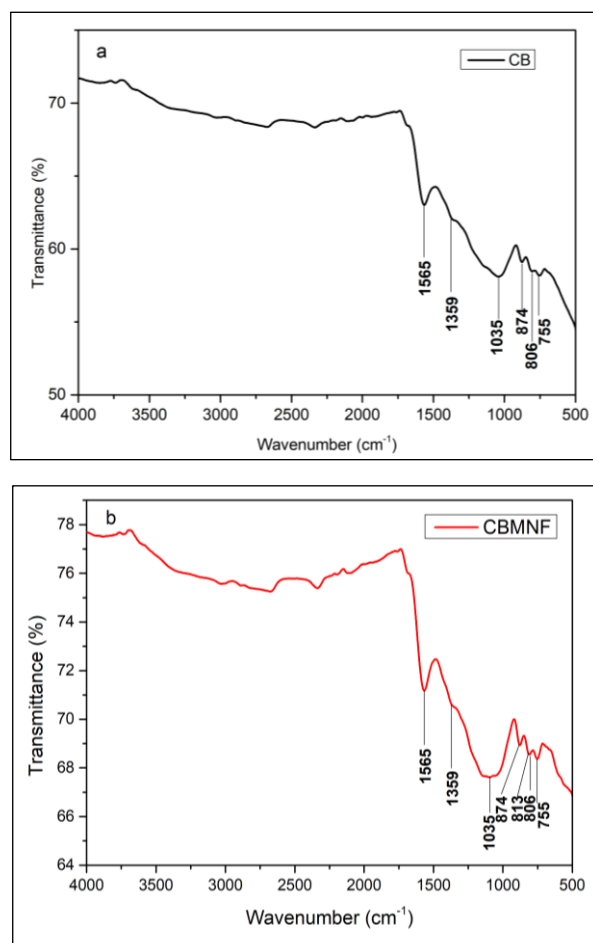


Fig. 2. FT-IR spectroscopy of (a) CB and (b) CBMNF

The FT-IR spectra of CBMNF was depicted in Fig. 2b. Similar to CB, CBMNF demonstrated a broad peak between 3600 – 3400 cm^{-1} , assigned to

the hydroxyl groups (OH) originating from polymeric alcohol, phenol and carboxylic groups. It is also noted that changes in peak position and intensity served to distinguish nutrient-loaded biochar from regular biochar, indicating a subtle shift in peak location and varying peak intensities. This alteration in CBMNF spectra might attribute to the integration of nutrients into CB structure. Specifically, new peaks at 813 cm^{-1} were observed in CBMNF spectra, possibly indicating the presence of incorporated metal-ligand bonds, given that spectral bands within the $1000\text{ to }700\text{ cm}^{-1}$ range are commonly associated with metal ligands such as M–O or M–O–H [37].

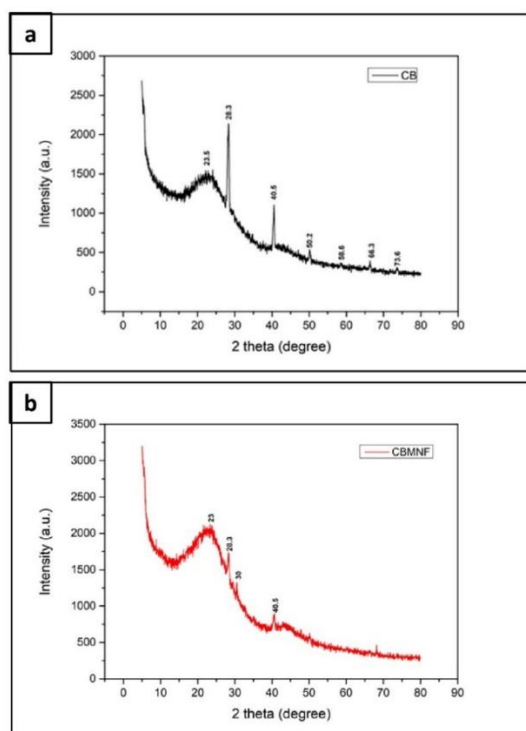


Fig. 3. XRD analysis of (a) CB and (b) CBMNF

The XRD pattern of CB is illustrated in Fig. 3a. The presence of crystalline inorganic fraction is suggested by the sharp peaks in the XRD patterns, while the diffused wide bands indicate the presence of short-range order in the biochar. The C (002) diffraction peak was identified as the one with a centre at around 2θ 23.5. Sharp peaks seen at 2θ values 28.3, 40.5, 50.2, 58.6, 66.3 and 73.6 could be assigned to KCl (sylvite-Ref. No. 00-041-1476) [41, 42].

In the XRD spectra of CBMNF (Fig. 3b), a prominent broad peak centered around 2θ value 23

was observed, showing greater intensity compared to CB. Additionally, the peaks associated with KCl at 2θ values of 28.3 and 40.5 exhibited reduced intensities. An additional peaks, observed at 2θ values 30 may be attributed to SiO_2 .

The CB and CBMNF were assessed by TGA study, which examined how the material's physical and chemical characteristics changed as the temperature rose. The TGA and differential thermogravimetry (DTG) interlinked thermogram of CB (Fig. 4a) showed that about 10-12 % of mass was lost during the first phase (from the initial temperature to $100\text{-}120^\circ\text{C}$). This was due to the loss of moisture or free and non-structural water and other volatile matter from surface or pores of the material. The loss of mass in the second phase, from 121.9°C to 399.2°C , was attributed to the the oxidation of cellulosic materials by heat. The thermal oxidation of more resistant organic structures, such as lignin, and thermally generated carbonized/aromatic structures resulted in the third phase, where overlapping weight loss centred around 350°C is observed. This process may have involved the release of gases, such as CO_2 , CO , and CH_4 [43, 44]. The recalcitrance index (R_{50}) value for CB was determined to be 0.467, slightly below 0.5. This suggests that the biochar is susceptible to degradation, and is not environmentally recalcitrant.

The TGA and DTG interlinked thermogram of CBMNF is given in Fig. 4b. In the thermogram of CBMNF, during the first phase, from 30°C to about 100°C , a 5 to 10 % reduction in weight was observed. This was attributed to moisture loss. Subsequently, when the temperature rose approximately to 350°C , the mass exhibited consistent stability, indicating the absence of free water molecules within the material. Between 300°C and 550°C , a significant mass reduction exceeding 50-60 % was observed, likely attributable to the decomposition of organic compounds. The final yield of CBMNF was determined to be in the range of 10-15 %. Beyond 550°C up to 750°C , there was no further change in mass, indicating that only the ash has remained. Also, the shifting of derivative thermo gravimetric (DTG) curve of CBMNF towards a wider range of temperatures depicted higher stability of the nutrient loaded biochar than the normal biochar. Upon adsorbing nutrient mix, an increase in R_{50} values to 0.543 was observed, indicating the improved stability of CBMNF.

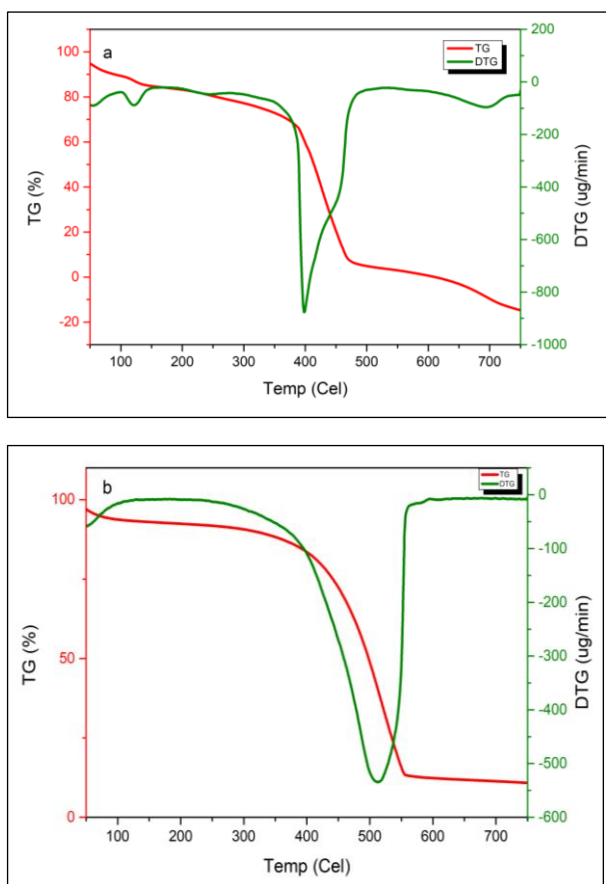


Fig. 4. TGA thermogram (green line) and DTG curve (blue line) of (a) CB and (b) CBMNF

Effect on soil water retention by addition of CBMNF

Soil enriched with CBMNF showed higher water retention than normal soil (Fig. 5), probably due to the decrease in the inter-particle pores. Addition of biochar improved the soil porosity allowing for higher water retention over an extended period [45].

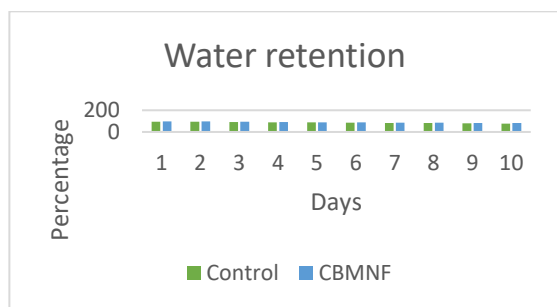


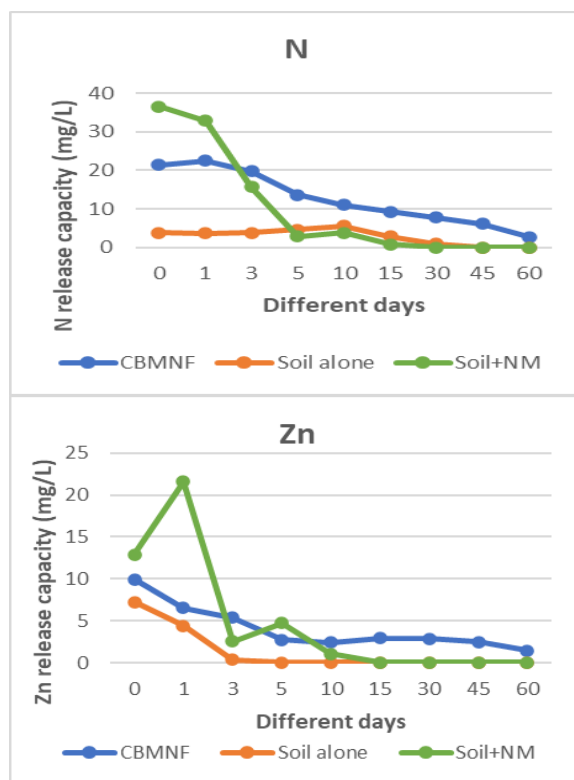
Fig. 5. Water retention by CBMNF

Slow release of nutrients in soil

The investigation analyzed the release patterns of essential nutrients, including N, Zn, Fe, Mn, Cu, B, and Mo, under various treatments. The results are shown in Fig. 6. The CBMNF treatment showed sustained NH_4^+ -N release until the 60th day, with concentrations decreasing over time, while both soil-

alone and soil+NM treatments ceased release by the 15th day. CBMNF also exhibited sustained Zn & Fe release throughout the experimental period, peaking on the first day and declining gradually thereafter, whereas soil-alone released these nutrients only up to the 5th day and soil+NM ceased release by the 10th day.

Continuous Mn release was observed under CBMNF treatment until the 60th day, while both soil-alone and soil+NM treatments ceased release by the third day. In the case of Cu, CBMNF showed continuous release, peaking from the 5th to 10th day, whereas soil-alone released Cu only on the first day, and soil+NM ceased release by the 3rd day. CBMNF sustained B release until the 60th day, while soil-alone and soil+NM treatments exhibited release for shorter durations. Additionally, a steady decrease in release of Mo was observed over time under all treatments, with CBMNF showing the most prolonged release. The initial spike in nutrient leaching observed in the case of Zn, Mn & B may be attributed to the release of loosely held surface-loaded nutrients. The subsequent delayed nutrient release of nutrients adsorbed in the pores of biochar. Mechanisms such as pore diffusion, ion interactions, and electrostatic forces influences nutrient adsorption and desorption on biochar. These findings underscore the potential of biochar-based slow-release fertilizers in extending nutrient availability over prolonged periods, offering insights for sustainable agricultural practices.



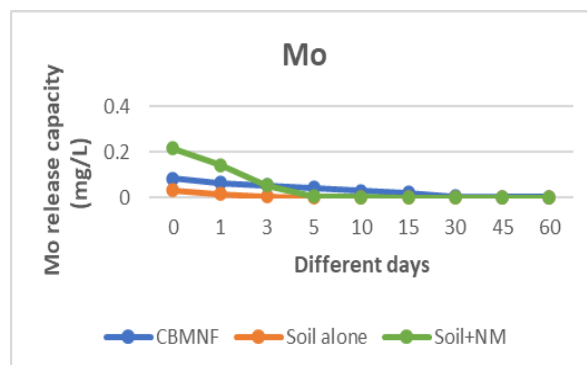
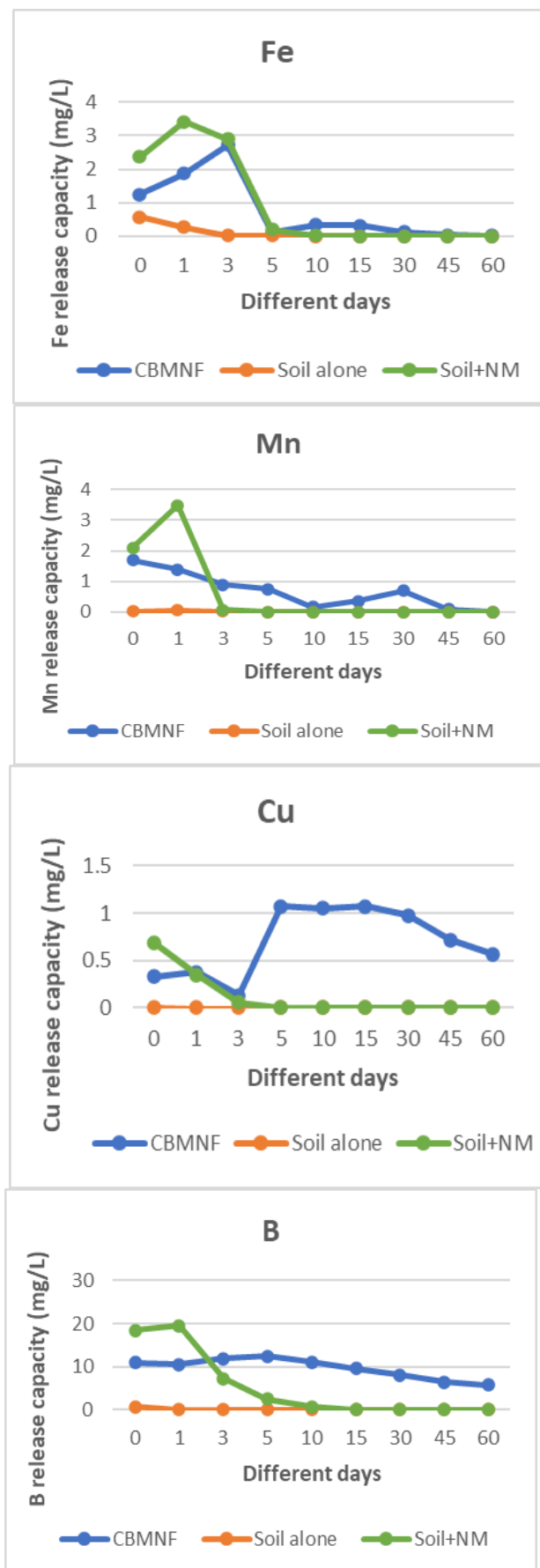


Fig. 6. Nutrient release patterns in soil

CONCLUSION

The coconut husk biochar has a honeycomb-like appearance with well developed porous structure as seen in the SEM images. The amorphous nature of biochar is confirmed by the diffuse broad bands observed in the XRD patterns. On incorporating the nutrients N, Zn, Fe, Mn, Cu, B and Mo into coconut husk biochar, the coconut biochar-based fertilizer (CBMNF) was synthesized. Comparison of FT-IR spectra of pristine biochar with that of CBMNF reveals a shift in the peak positions indicating changes in surface functional groups due to adsorbed nutrients. The deposition of nutrients within the pores of biochar is clearly visible in the SEM images of CBMNF. The XRD data of CBMNF were quite similar to those of CHB. A notable difference was the reduction in intensities of peaks assigned to inorganic entities like KCl, probably due to their loss during the impregnation process. TGA confirmed the higher stability of CBMNF than CHB. It also exhibited improved water retention. Additionally, studies on the nutrient release in soil revealed that CBMNF releases nutrients in a slow and sustained manner and acts as a slow-release fertilizer.

Author contribution: Methodology and original draft preparation by Aida Treasa Sojan, Supervision and formal analysis by John K. Smitha & interpretation of all analytical data critically reviewing the manuscript.

Funding: This research was funded by Kerala Agricultural University, Thrissur with order No. Acad(2) 331/2022 dated 15-12-2022.

Declaration: We wish to confirm that there are no known conflicts of interest associated with this publication.

This work was presented at the International Conference on Recent Advances in Waste Minimization and Utilization 2024.

Ethical approval: Not applicable

Informed consent: Not applicable

REFERENCES

1. P.M. Divya, B.S. Roopa, C. Manusha, P. Balannara, *J. Food Sci. Technol.* **60**,:441 (2023).
2. T.K. Hoe, *The Planter, Kuala Lumpur*, **94**, 413 (2018)..
3. R. Senthilkumar, *Asia Pacific J. Res.*, **1**, 34 (2015).
4. A.J. Atapattu, S.S. Udumann, T.D. Nuwarapaksha, N.S. Dissanayaka, (2024). Upcycling Coconut Husk By-Products: Transitioning from Traditional Applications to Emerging High-Value Usages. In: R. Neelancherry, B. Gao, A. Wisniewski Jr, (eds) *Agricultural Waste to Value-Added Products*. Springer, Singapore. https://doi.org/10.1007/978-981-97-2535-9_12.
5. M.P. Sujatha C. Lathika, J.K. Smitha, Sustainable and efficient utilization of weed biomass for carbon farming and productivity enhancement: a simple, rapid and ecofriendly approach in the context of climate change scenario. *Environ Challenges*, **4**, 100150 (2021). <https://doi.org/10.1016/j.envc.2021.100150>.
6. P. Dittakit, J. Singkham, W. Viriyasuthee, K. Sangmanee, *ASEAN J. Sci. Tech. Report*, **26**, 52 (2023).
7. M.Z. Hossain, M.M. Bahar, B. Sarkar, S.W. Donne, Y.S. Ok, K.N. Palansooriya, M.B. Kirkham, S. Chowdhury, N. Bolan, *Biochar*, **2**, 379 (2020).
8. E.M G.N.Ekanayaka, D.K.R.P.L. Dissanayake, S.S. Udumann, D.M.N.S Dissanayaka, Nuwarapaksha, T. D., Herath, H. M. S. K., A.J. Atapattu, 2023, *IOP Conference Series: Earth and Environmental Science*, 2023 (Vol. 1235, No. 1, p. 012009). IOP Publishing.
9. H.A. Khan, S.R. Naqvi, M.T. Mehran, A.H. Khoja, M.B.K. Niazi, D. Juchelkova, D., A. Atabani, *Chemosphere*, **285**: 131382 (2021).
10. S.K. Das, G.K. Ghosh, 2021. *Biomass Convers. Biorefin.* [e-journal]. Available: doi: <https://doi.org/10.1007/s13399-021-01880-5> [07 March 2022].
11. Z. Cen, L. Wei, K. Muthukumarappan, A. Sobhan, R. McDaniel, *J. Soil Sci. Plant Nutr.*, **21**, 2007 (2021).
12. C.F. Barbosa, D.A. Correa, J.S.D.S. Carneiro, L.C.A. Melo, *Sustain.* [e-journal] **14**, (2). Available: <https://doi.org/10.3390/su14020686> [28 Dec. 2022].
13. J.K. Smitha, A.T. Sojan, K. Arhana, T. Geetha, Biochar-Based Fertilizers: A Smart Solution for Sustainable Agriculture. In: Neelancherry, R., Gao, B., Wisniewski Jr, A. (eds) *Agricultural Waste to Value-Added Products*. Springer, Singapore. https://doi.org/10.1007/978-981-97-2535-9_8. 2024
14. W. Gwenzi, T.J. Nyambishi, N. Chaukura, N. Mapope, *Int. J. Environ. Sci. Technol.*, **15**, 405 (2018)..
15. M.A. Khan, K.W. Kim, W. Mingzhi, B.K. Lim, W.H. Lee, J.Y. Lee, *Environ.* **28**, 231 (2008)..
16. Y. Lee, J. Park, C. Ryu, K.S. Gang, W. Yang, Y.K. Park, J. Jung, S. Hyun, *Bioresour. Technol.*, **148**, 196 (2013).
17. S. Rajkovich, A. Enders, K. Hanley, C. Hyland, A.R. Zimmerman, J. Lehmann, *Biol. Fertil. Soils*, **48**, 271 (2012).
18. M.L. Jackson, *Soil Chemical Analysis*. Prentice Hall of India (Pvt.) Ltd., New Delhi, 1973. P. 498.
19. A.Z.A. Hassan, A.W.M. Mahmoud, Hydrothermal Synthesis of Nano Crystals (AM). *J. Nanomater. Mol. Nanotechnol.*, **4**, 7 (2015).
20. H. Gong, Z. Tan, L. Zhang, Q. Huang (2019).. *Sci. Total Environ.* [e-journal] 694. Available: <https://doi.org/10.1016/j.scitotenv.2019.133728> [20 July 2022].
21. K.W. Jung, M.J. Hwang, K.H. Ahn, K. H., Y.S. Ok, *Int. J. Environ. Sci. Technol.* **12**, 3363 (2015).
22. S. Jiang, T.A. Nguyen, V. Rudolph, H., Yang, D. Zhang, Y.S. Ok, L. Huang, 2017 *Environ. Geochem. Health*, **39**, 403 (2017).
23. Y. Dai, W. Wang, L. Lu, L. Yan, D. Yu, *J. Clean. Prod.* **257**, 120573 (2020).
24. F.N. Mukome, X. Zhang, L.C., Silva, J. Six, S.J. Parikh, *J. Agric. Food Chem.*, **61**, 2196 (2013).
25. B. Singh, M.M. Dolk, Q. Shen, M. Camps-Arbestain, Biochar pH, Electrical Conductivity and Liming Potential. In B. Singh, M. Camps-Arbestain, & J. Lehmann (Eds.), *Biochar: A Guide to Analytical Methods* (2017). CSIRO Publishing. Pp. 23-28. <https://doi.org/10.1071/97814863051003>.
26. X. Zhang, P. Zhang, X. Yuan, Y. Li, L. Han, *Bioresour. Technol.* **296**, 122318 (2020).
27. S.P. Sohi, E. Krull, E. Lopez-Capel, R. Bol, 2010. A review of biochar and its use and function in soil. *Adv. Agron.*, **105**, 47 (2010).
28. S. Wang, B. Gao, A.R. Zimmerman, Y. Li, L. Ma, W.G. Harris, K.W. Migliaccio, *Chemosphere* **134**, 257 (2015).
29. L. Zhang, Y. Ren, Y. Xue, Z. Cui, Q. Wei, C. Han, J. He, *RSC Adv.* **10**, 35878 (2020).
30. A.A. Oyekanmi, A.A. Latiff, Z. Daud, R.M. Saphira, N. Ismail, A. Aziz, M. Rafatullah, K. Hossain, A. Ahmad, A. Kamoldeen, *Int. J. Environ. Anal. Chem.* **99**, 707 (2019).
31. F.R. Amin, Y. Huang, Y. He, R. Zhang, G. Liu, C. Chen, *Clean Technol. Environ. Policy*, **18**, 1457 (2016).
32. S. Li, G. Chen, *Waste Manag.* **78**, 198 (2018)..
33. B.C. Lago, C.A. Silva, L.C.A. Melo, E.G. de Moraes (2021). *Sci. Total Environ.* [e-journal] 794. Available: <https://doi.org/10.1016/j.scitotenv.2021.148762> [11 May 2022].
34. H. Bamdad, K. Hawboldt, *Can. J. Chem. Eng.* **94**, 2114 (2016).
35. M.F.P. Ferreira, B.F.H. Oliveira, W.B.S. Pinheiro, N.F. Correa, L.F., Franca, N.F.P. Ribeiro (2020). *Biomass Bioenerg.* [e-journal] 140. Available: <https://doi.org/10.1016/j.biombioe.2020.105707> [19 May 2022].
36. H. Ullah, Q. Abbas, M.U. Ali, A.I. Cheema, B. Yousaf, J. Rinklebe, J. 2019. *Chem. Eng. J.* **373**, 44 (2019).

37. B. Zhao, O.D. Nartey, Characterization and evaluation of biochars derived from agricultural waste biomasses from Gansu, China. In: *Proceedings of the World Congress on Advances in Civil, Environmental, and Materials Research*, 24-28 August 2014, Busan, Republic of Korea.
38. D. Pattnaik, S. Kumar, S.K. Bhuyan, S.C. Mishra, Effect of carbonization temperatures on biochar formation of bamboo leaves. In: *IOP Conference Series: Materials Science and Engineering* 338(1): 012054, 2018.
39. H. Wang, D. Chen, J. Xu, R. Sun, Y. Liu, Y. Zhang, R. Xu, *Soc. Sci. Res. Network* [online]. Available: <https://dx.doi.org/10.2139/ssrn.4091168> [23 Oct. 2022].
40. E. Doelsch, A. Masion, J. Rose, W.E. Stone, J.Y. Bottero, P.M. Bertsch, 2003.. *Colloids Surf. A: Physicochem. Eng. Asp.* **217**, 121 (203).
41. A.M. Dehkhoda, N. Ellis, N., E. Gyenge, *J. Appl. Electrochem.*, **44**, 141 (2014).
42. Y. Yan, S. Manickam, E. Lester, T. Wu, C.H. Pang (2021). *Ultrason. Sonochem.* [e-journal] **73**. Available: <https://doi.org/10.1016/j.ultsonch.2021.105519> [22 Jan. 2022].
43. O.R. Harvey, L.J. Kuo, A.R. Zimmerman, P. Louchouart, J.E. Amonette, B.E. Herbert, *Environ. Sci. Technol.* **46**, 1415 (2012).
44. C.T. Chong, G.R. Mong, J.H. Ng, W.W.F. Chong, F.N. Ani, S.S. Lam, H.C. Ong, 2019. Pyrolysis characteristics and kinetic studies of horse manure using thermogravimetric analysis. *Energy Convers. Manag.* **180**, 1260 (2019).
45. E.O. Ndede, S. Kurebito, O. Idowu, T. Tokunari, K. Jindo, *Agronomy*, **12**, 11 (2022)..